Applied Radiation and Isotopes 190 (2022) 110462

Contents lists available at ScienceDirect

Applied Radiation and Isotopes

journal homepage: www.elsevier.com/locate/apradiso

Thermoluminescence studies of calcite conducted by bacterial $CaCO_3$ precipitation in organic soil

Hüseyin Toktamış [a,*], Muhammed Hatib [a], H. İbrahim Kılıç [b], Hanifi Çanakçı [c]

[a] University of Gaziantep, Department of Engineering Physics, Gaziantep, Turkey
[b] University of Gaziantep, Department of Biology, Gaziantep, Turkey
[c] Hasan Kalyoncu University, Department of Civil Engineering, Gaziantep, Turkey

ARTICLE INFO

Keywords:
Thermoluminescence
Calcite
Bacterial calcium carbonate ($CaCO_3$) precipitation

ABSTRACT

In this study, the thermoluminescence (TL) properties of the calcite conducted by bacterial calcium carbonate ($CaCO_3$) precipitation (BCCP) in organic soils were investigated. The bacterial calcium carbonate ($CaCO_3$) precipitation (BCCP) is a popular technique and has been applied in a variety of civil and geotechnical engineering applications. For example, bacterial calcium carbonate precipitation fills the gaps on the organic ground and makes cementing it with the biological method using bacteria. The study reveals that the calcium carbonate mineral called as calcite has a clear TL glow curve with four main peaks located around 90, 140, 210 and 240 °C, a wide linear dose response region between 140Gy and 2.3 kGy is observed. In addition, a good reusability is seen in the high temperature peaks. The TL glow curve peaks are not affected by reusability. Although the dosimetric peaks at 210 and 240 °C appear to be nearly constant, the TL peak intensities at 90 °C and 140 °C completely faded after 24 and 336 h storage time, respectively. The activation energies (E_a) and frequency factors (s) for peaks at 90 °C, 140 °C, 210 °C and 240 °C were evaluated via variable heating rate (VHR). The activation energy of the peaks in the TL glow curve is lying between 0.57eV and 1.04 eV.

1. Introduction

Biomineralization is a phenomenon of chemical alteration in the environment that results in the precipitation of minerals by microbiological organisms (Barkay and Schaefer, 2001; Phillips et al., 2013; Stocks-Fischer et al., 1999). This leads to the formation of various biological minerals and there are more than sixty species that occur as extracellular or intracellular inorganic crystals (Dhami et al., 2013; Konishi et al., 2006; Yoshida et al., 2010). In all groups of living organisms, extracellular mineralization is the best known mineralization, and carbonate precipitation is an example of extracellular mineralization (Lowenstam, 1981). Trace elements of organic compounds found in crystals can regulate the biomineralization process (Yoshida et al., 2010). There are several ways to generate biominerals such as biologically controlled mineralization (Benzerara et al., 2011; Lowenstam and Weiner, 1989; Phillips et al., 2013), biologically influenced mineralization (Benzerara et al., 2011; Phillips et al., 2013) and biologically induced mineralization (De Muynck et al., 2010; Lowenstam and Weiner, 1989; Phillips et al., 2013; Stocks-Fischer et al., 1999).

Bacterial calcium carbonate precipitation (BCCP) is a process for the formation of calcium carbonate from a supersaturated solution due to the presence of its microbial cells and biochemical activities (Bosak, 2011). During this process, organisms are able to secrete one or more metabolites (CO_3^{2-}) that react with ions (Ca^{2+}) in the environment resulting in the subsequent precipitation of minerals.

Bacterial cells are very important in the precipitation of $CaCO_3$, because bacteria provide nucleation sites (heterogeneous nucleation) and influence the specific types of minerals formed (Douglas and Beveridge, 1998; Rodriguez-Navarro et al., 2012).

Urease is an enzyme that catalyzes the hydrolysis of urea into ammonium and carbonate. During the formation of calcite precipitation, the chemical processes are described in the equations (Anbu et al., 2016):

$$CO(NH_2)_2 + H_2O \rightarrow NH_2COOH + NH_3 \quad (1)$$

$$NH_2COOH + H_2O \rightarrow NH_3 + H_2CO_3 \quad (2)$$

$$H_2CO_3 \leftrightarrow HCO_3^- + H^+ \quad (3)$$

$$2NH_3 + 2H_2O \leftrightarrow 2NH_4^- + 2OH^- \quad (4)$$

* Corresponding author.
E-mail address: toktamis@gantep.edu.tr (H. Toktamış).

https://doi.org/10.1016/j.apradiso.2022.110462
Received 13 June 2022; Received in revised form 11 September 2022; Accepted 12 September 2022
Available online 16 September 2022

$$HCO_3^- + H^+ + 2OH^- \leftrightarrow CO_3^{2-} + 2H_2O \quad (5)$$

$$Ca^{2+} + \text{Bacterial cell} \rightarrow \text{Cell-}Ca^{2+} \quad (6)$$

$$\text{Cell-}Ca_2 + CO_3^{2-} \rightarrow \text{Cell-}CaCO_3 \quad (7)$$

Thermoluminescence (TL) is a luminescence phenomenon of an insulator or semiconductor that can be observed when the solid is thermally stimulated (Bos, 2007). It is a stimulated emission process that occurs due to the thermally excited light emission after prior absorption of energy from an external ionizing radiation source (alpha, beta, gamma radiation) releasing electrons through the crystal lattice and trapping some of them in imperfections of the lattice (Chen and McKeever, 1997). Subsequent heating of the crystal allows some of these trapped electrons to escape in the form of emission light (Claudio, 2003; Pagonis et al., 2006). There are many types of calcite minerals in the natural environment, have colors red, gray, green, blue, brown, yellow and orange, but if its color close to white that refer to the high purity.

Calcium carbonate ($CaCO_3$) emits intense thermoluminescence (TL). Based on this result, it is used to date both inorganic carbonates and biogenic calcite produced by marine organisms (Duller et al., 2009). Biogenic calcium carbonates contain organic components of the shell mixed into the calcite structure. During TL measurement, heating of the samples causes combustion of these organic compounds, which affects the measurement of the dose-dependent TL signal from the calcite. Duller et al. (2009) studied two types of biogenic with a high degree of mineralization: slug plates and snail opercula. These two types of biogenic carbonates are commonly found in archaeological and geological sediments in areas with a carbonate-rich bedrock.

The thermoluminescence emissions, observed in insulator materials during excitation with temperature, depend on all intrinsic and/or extrinsic defects. These defects determine the presence of thermoluminescence trapping and recombination sites (Garcia-Guinea et al., 2009a). Calcite (trigonal) can modify its spatial structure giving rise to aragonite (orthorhombic) and, on the other hand, the chemical composition since Ca(II) can be replaced in the lattice by divalent cations of Sr(II) or Zn(II) giving rise to strontianite or smithsonite, respectively, showing significant luminescence emission (Tatumi et al., 1993; Garcia-Guinea et al., 2009a, 2009b). TL emission spectra at longer wavelengths, from 600 to 650 nm, are reported for a wide range of carbonates and are associated with Mn^{2+} luminescence centres. The emission wavelengths of Mn show monotonic dependencies in rhombohedral phases as a function of metal-oxygen bond length in different carbonate phases (Calderon et al., 1996).

The TL glow curve of calcite ($CaCO_3$) has peaks at 100 °C, 270 °C, and 340 °C with the strongest emission in the red part of the spectrum; many of these emissions are associated with a Mn^{2+} defect (Krbetschek et al., 1997). Mn^{2+} is considered the main recombination centre for calcites (Polikreti et al., 2003).

The study of TL properties has been investigated for many types of calcite with many different radiation sources (García-Guinea et al., 2015; Isik et al., 2021; Toktamış et al., 2016; Toktamiş et al., 2014; Valle-Fuentes et al., 2007; Yildirim et al., 2012). In general, they concluded that calcite exhibits thermoluminescence properties with three distinct peaks located at 100 °C–150 °C, 200 °C–300 °C, and 310 °C–400 °C temperature intervals, showing strong linearity of dose response.

In an insulator, the transitions of electron and holes between conduction band, valence band and some energy levels inside forbidden band gap are described by some differential equations and the numerical solutions of the these equations can help in the understanding of the physical mechanisms governing thermoluminescence (TL) emission (Gómez-Ros et al., 2006). However they are not easy to analyse the complex experimental TL glow curve. The general order kinetics (GOK) and mixed order kinetics (MOK), known as approximated equations, are widely used for practical purposes and overcome this difficulty (Gómez-Ros and Kitis, 2002; Horowitz and Yossian, 1995). There are several methods to analyse the TL glow curve and evaluate kinetic parameters of traps such as Variable heating rate (VHR), Initial rise (IR), Peak shape (PS), Computer glow curve deconvolution (CGCD), Isothermal decay (ID), and three point method (TPM). The commonality of these techniques is the use of the TL glow curve in the evaluation of kinetic parameters. In the VHR method, the variation of TL peak temperature (T_m) as a function of heating rate (β) is used. From the plot of ln (T_m^2/β) versus $1/T_m$ of any TL peak, activation energy (E_a) and frequency factor (s) are easily found by using slope and intercept of the plot. When a TL glow curve includes small satellite peaks surrounding the main peak, the VHR method becomes very useful for calculating the kinetic parameters because it has little effect on the accuracy of the kinetic parameters. However, the TL curve does not match the actual peak maxima, and this method does not provide accurate results for the kinetic parameters when multiple glow peaks overlap (Topaksu et al., 2015). In the IR method, all relevant occupancies of the states can be considered as being approximately constant at low temperature end of the peak. Two kinetic parameters (E_a and s) are calculated from the plot of ln (I) versus 1/T. By using PS method, the order of kinetics *b* can be estimated by means of shape parameter of TL glow curve. The CGCD method has the advantage over experimental methods without resorting to heat treatment. In this method the TL glow curve is fitted to the several satellite peaks. In the TPM method, three points are choosen in the TL glow curve and the kinetics order (b) and other kinetic parameters are determined, successively. In the ID method, the TL sample temperature is kept constant and the light emission can be recorded as a function of time. The light emission will decay exponentially with time *t* and a plot of *ln (I)* against t will give a straight line. The experiments are carried out at two different constant temperatures T_1 and T_2, resulting in two different slopes. By using two slopes, activation energy is found. In fact, the result of CGCD method is not physically acceptable and it depends on the shape of peak. On the contrary, the IR and VHR methods don't depend on the shape of peak (Claudio, 2003).

2. Preparation of samples and equipments

2.1. Preparation of samples

All samples were natural calcite minerals produced by BCCP, i.e. bacterial precipitation of calcium carbonate ($CaCO_3$) (Sıdık et al., 2015). In general, calcite is the most widespread soil carbonate growing in root zones with high CO_2 density and derived from calcareous parent materials (Schaetzl and Anderson, 2005). Microbial calcite can be formed by complex biochemical interactions, such as the interaction between Bacillus Pasturii, ammonia and urease. The production of urease depends on the activity of microorganisms in alkalophilic soils. This microorganism hydrolyzes urea to produce carbon dioxide (CO_2) and ammonia (NH_3) which raise the PH in the soil high and subsequently prepare conditions in the organic soil for the production calcium carbonite ($CaCO_3$) (DeJong et al., 2010) as shown in Fig. 1.

2.2. Equipments

Samples were weighed to 15 mg using a digital balance. The samples were irradiated with beta rays (β-rays) source at room temperature using a calibrated ^{90}Sr–^{90}Y source. The activity of this radiation source is 100 mCi. The typical strength of a 100 mCi Sr^{90} β-source installed in a 9010 Optical Dating System is 2.64 Gy/min (0.0438 Gy/s). The irradiation equipment is an additional part of the 9010 optical dating system purchased from Little More Scientific Engineering, UK. After the samples were exposed to the beta radiation source, they were read out by a Harshaw QS 3500 manual reader (TLD reader) connected to PC, and the TL glow curve which gives the variation of TL light as a function of temperature was obtained. A standard clear glass filter was always installed in the reader between the planchette and the photomultiplier

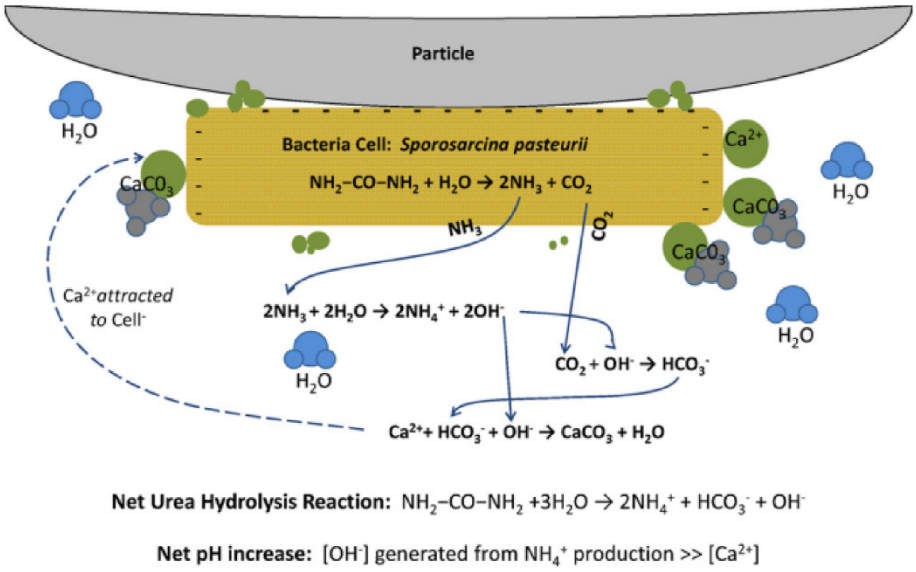

Fig. 1. Diagram of bio-mediated calcite precipitation using ureolysis (DeJong et al., 2010).

tube to eliminate the infrared light emitted from the reader and the samples.

Photomicrographs of the sample were taken with the ZEISS - Gemini SEM 300 at the Central Laboratory of Gaziantep University. The magnification ranges from 12x to 2000000x and the accelerating voltage ranges from 5 kV to 30 kV. The resolution is 0.6 nm at 30 kV. Its magnification is from 12x to 2000000x and its acceleration voltage is 30 kV. The resolution is 0.6 nm at 30 kV.

3. Experimental procedures

In this study, four experiments are performed: Dose Response, Heating Rate, Reusability or Repeatability and Fading. Samples weighing approximately 15 mg were used in all experiments. Before each irradiation procedure, all aliquots were readout to determine the background and subtracted from the main TL measurement. In the dose response part, 15 mg samples (10 aliquots) were irradiated with different dose levels (from 2.4Gy to 6.9 kGy) and read out at a heating rate of 1 °C/s of heating rate from room temperature to 400 °C. For the heating rate part, 15 mg samples (5 aliquots) were weighed, then irradiated with 36 Gy from a beta source and finally read out at five different heating rates of 1, 2, 3, 4 and 5 °C/s. In the fading part, 15 mg samples (7 aliquots) were stored in a darkroom at room temperature for different storage times (15min, 1 h, 8 h, 24 h,120 h and 336 h) as soon as irradiated 36Gy radiation dose. At the end of the storage time, each sample was readout at 1 °C/s. In the reusability part, the 15 mg sample (one aliquot) was irradiated with 36 Gy and read out with the TLD reader at 1 °C/s and repeated eight times.

4. Results and discussions

4.1. SEM analysis

The SEM images of the organic soil before and after BCCP are shown in Fig. 2 (a) and (b). The images show $CaCO_3$ crystals on the surface of the organic soil particles (Sıdık et al., 2015).

The results of scanning electron microscopy (SEM) show, as shown in Fig. 2 (b), that the precipitated calcium carbonate fill the voids between the sand particles after treatment.

4.2. Dose response

15 mg samples (10 aliquots) were irradiated with different doses (from 2.4Gy to 6.9 kGy) and read out at a heating rate of1°C/s from room temperature to 400 °C. The obtained TL glow curves are shown in Fig. 3.

In Fig. 3, TL glow curves of calcite mineral for different dose levels (from 2.4Gy to 6.9 kGy) were given. There are four TL peaks located around 90, 140, 210 and 240 °C. At higher applied doses (bigger than 576 Gy), a new TL peak around 340 °C is appeared and the low

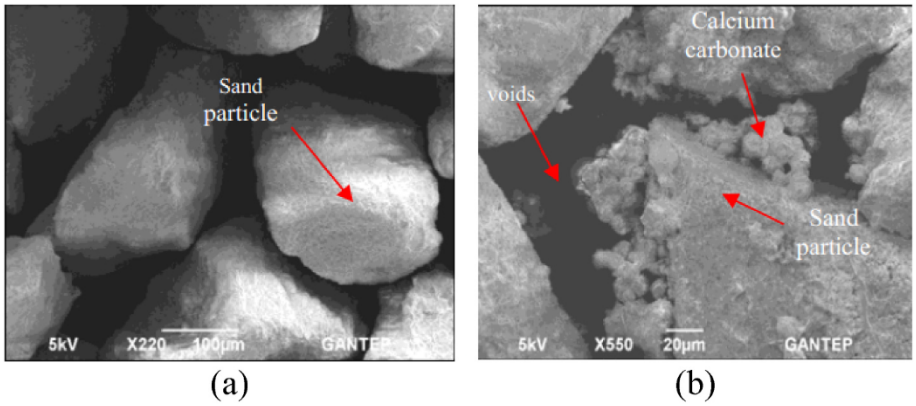

Fig. 2. Organic soil particles a) before treatment b) after treatment (Sıdık et al., 2015).

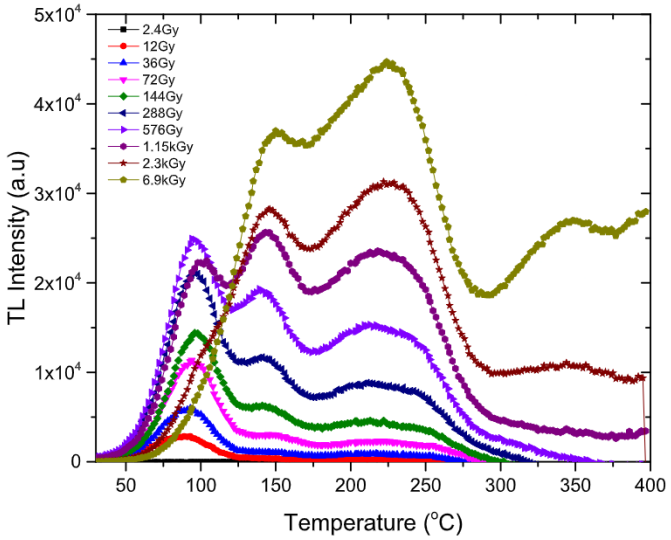

Fig. 3. TL glow curves of calcite mineral for different dose levels (from 2.4Gy to 6.9 kGy).

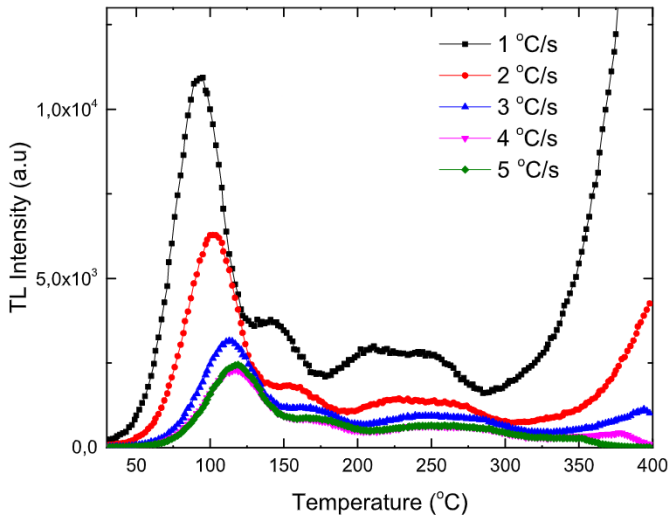

Fig. 5. TL glow curves of calcite mineral for different heating rates (from 1 °C/s to 5 °C/s).

temperature TL peak around 90 °C is completely disappeared. The TL peaks at 210 °C and 240 °C are converged and merged in one peak at temperature ~225 °C.

Fig. 4(a) and (b) show the variations in TL peak temperatures and area under the TL glow curve at different applied dose levels, ranging from 2.4 Gy to 6.9 kGy. The TL peak temperatures are stable at different doses. The area under the TL glow curve increases linearly between 144Gy and 2.3 kGy.

4.3. Heating rate experiment

The heating rate represents the dynamic factor which effected on the characteristics of TL glow curve of the studied samples. First, 15 mg samples (5 aliquots) were weighed, then irradiated with 36Gy from a beta source and finally read out at five different heating rates of 1, 2, 3, 4 and 5 °C/s.

In the results of the heating rate experiment, the shape of the TL glow curve doesn't change at different heating rates as seen in Fig. 5, but the position of the TL peaks and their intensity change. The variations of TL peak positions and normalized area under the TL glow curve can be seen in Fig. 6 (a) and (b).

In Fig. 6 (a), the TL peak located around 90 °C shifted to higher temperature region about 28 °C between 1 and 5 °C/s heating rate. The shifts of TL peaks located around 140 °C, 210 °C and 240 °C are 26 °C, 33 °C, and 47 °C, respectively. All of these changes occur while the shape of the TL glow curve for calcite remains constant. In Fig. 6 (b), the area under the TL glow curve decreases by 60% and 70% at 2 °C/s and 3 °C/s, respectively. Finally, it becomes almost constant at 4 °C/s and 5 °C/s.

4.4. Fading experiment

Fading experiment is one of the necessary studies in dosimetric research. In this experiment, the irradiated sample is waited at different storage times and read out. With this experiment, it is observed whether the TL signal decreases with storage time or not. In the current study, 15 mg samples (7 aliquots) were kept in a darkroom at room temperature for different storage times (15min, 1 h, 8 h, 24 h,120 h and 336 h) as soon as irradiated 36Gy radiation dose. At the end of the storage period, each sample was readout at 1 °C/s.

The variation of the TL glow curve as a function of storage time is given in Fig. 7. The TL peak intensities at 90 °C and 140 °C faded completely after 24 and 336 h storage time, respectively.

A stability was observed for TL peak temperatures of peaks located around 90, 140, 210 and 240 °C as a function of storage time as shown in Fig. 8 (a). In Fig. 8 (b), TL glow curve is divided into two main regions which are 30–150 °C and 150–400 °C. While the area between 150 and 400 °C seems almost constant, the area between 30 and 150 °C decreases

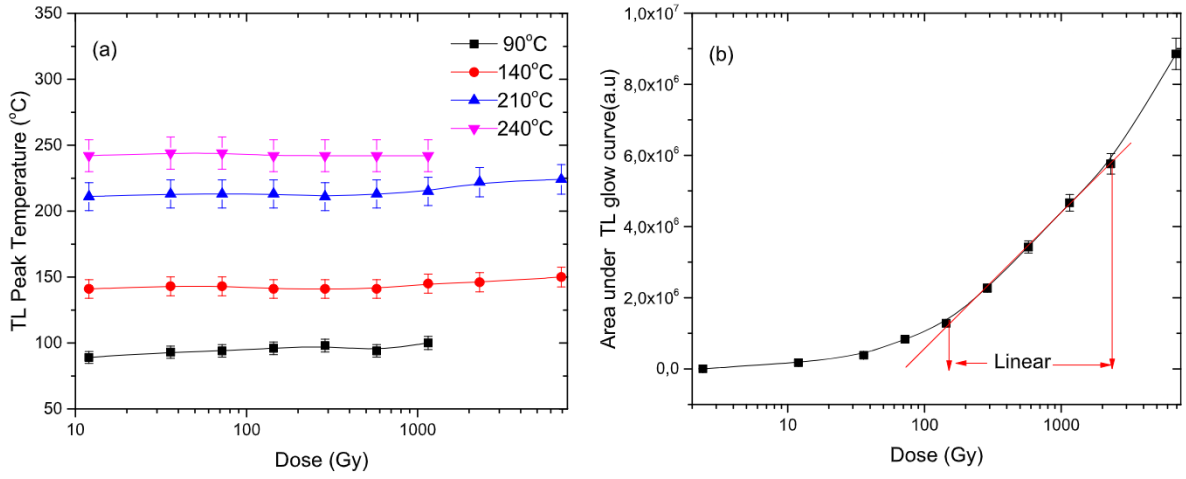

Fig. 4. The effect of applied dose on (a) TL peak temperatures and (b) area under the TL glow curve.

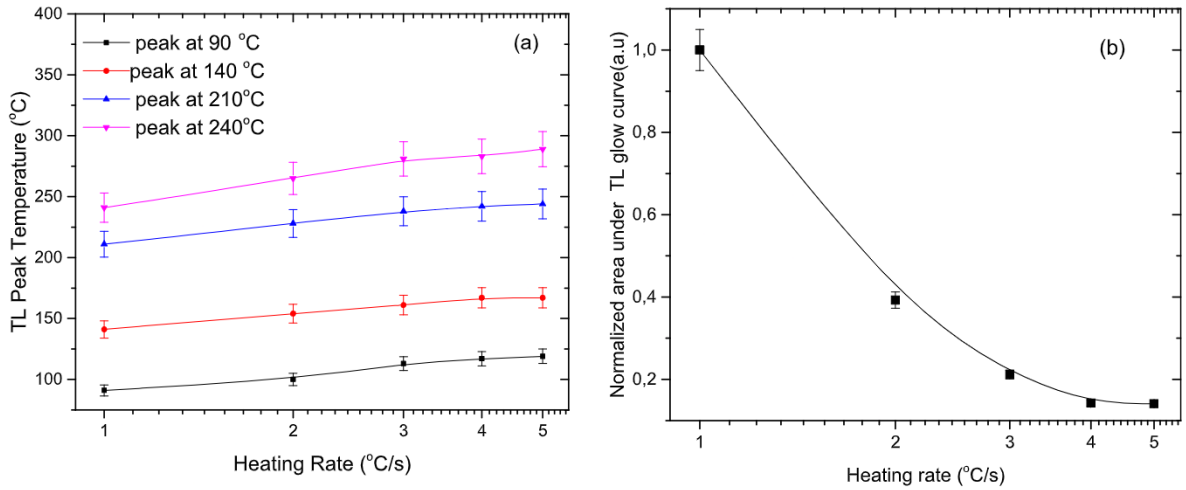

Fig. 6. Variation of (a) TL peak temperatures and (b) normalized area under the TL glow curve as a function of heating rate (from 1 °C/s to 5 °C/s).

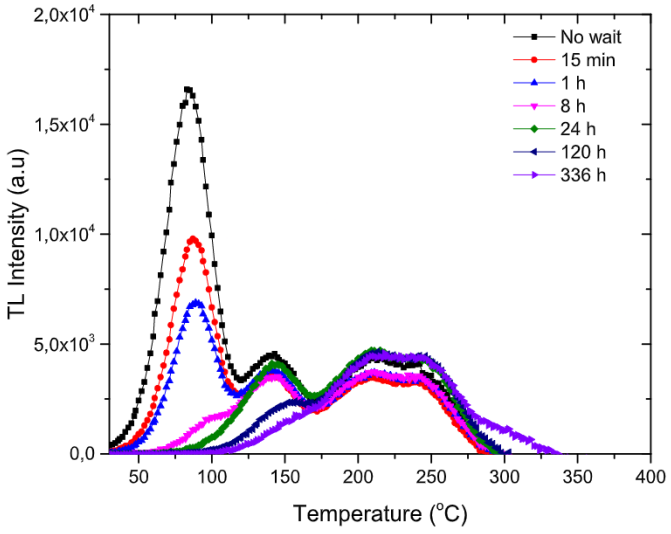

Fig. 7. The variation of TL glow curve as a function of storage time.

suddenly up to 100 min of storage time and finally faded completely.

4.5. Reusability experiment

Reusability or repeatability experiment is a necessary part of dosimetric purposes. In this experiment, the 15 mg sample (one aliquot) was irradiated with 36 Gy and read out by TLD reader at 1 °C/s and repeated eight times. The result is that no additional distinct peak appears at the end of each cycle, as shown in Fig. 9.

As can be seen from Fig. 10(a), there is no significant shift in the temperature peaks. The standard deviation was calculated as 1%, 0.69%, 0.73%, and 0.58% for the TL peak temperatures at 90, 140, 210, and 240 °C, respectively.

The TL peak intensities at 140, 210, and 240 °C are more stable than the TL peak intensities at 90 °C, as shown in Fig. 10(b). In addition, the standard deviation for the TL peak intensities of the peaks at 90, 140, 210, and 240 °C were calculated to be 5.7%, 5.8%, 9.3%, and 9.8%, respectively.

4.6. Kinetic parameters via variable heating rate (VHR) method

Activation energy (E_a) and frequency factor (s) are two kinetic parameters of the trap in a dosimetric material. Activation energy, also called as trap depth, is the difference in energy between the trap and the bottom of the conduction band. The term of frequency factor, also called as attempt-to-escape frequency, represents the number of times per

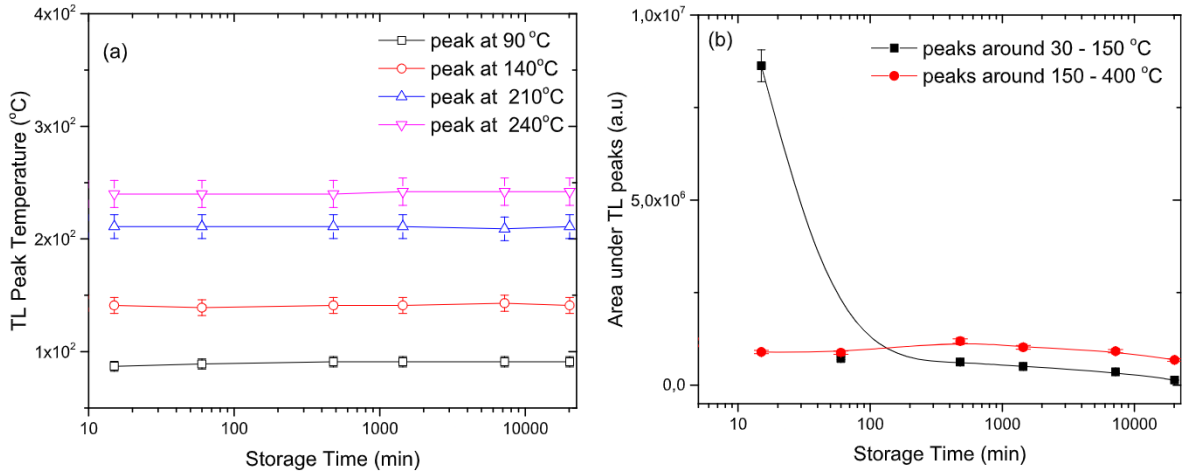

Fig. 8. The variation of (a) TL peak temperatures and (b) area under the selected TL peaks as a function of storage time.

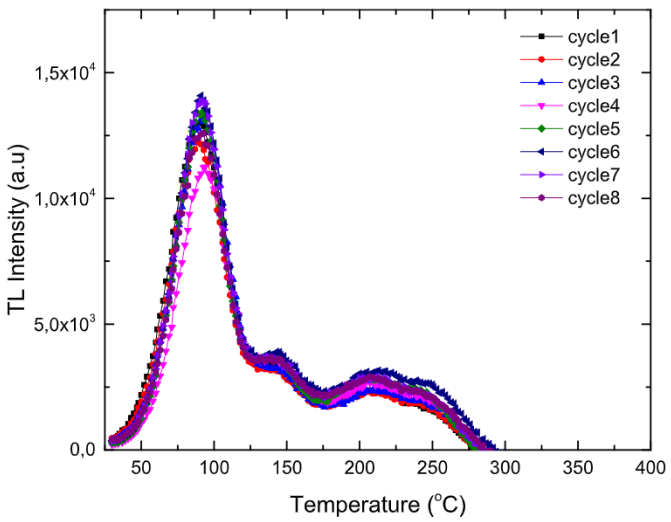

Fig. 9. The variation of TL glow curve as a function of cycle of measurement.

second that a bound electron interacts with the lattice phonons times a transition probability (McKeever, 1985).

Fig. 11 shows the plot of ln (T_m^2/β) versus $1/T_m$ of (a) peak at 90 °C, (b) peak at 140 °C, (c) peak at 210 °C and (d) peak at 240 °C. According to the variable heating rate (VHR) method, the slope of the graph gives the ratio E_a/k and the intercept gives the ln (sk/E_a) to evaluate the activation energy (E_a) and frequency factor (s). The variable heating rate (VHR) method can be used to understand how traps are emptied at different heating rates while holding all other parameters constant (Topaksu et al., 2015). The relationship between heating rate (β) and peak temperature (T_m) is given in equation (8) (Claudio, 2003):

$$\frac{\beta E_a}{kT_m^2} = s.\exp\left(-\frac{E_a}{kT_m}\right) \quad (8)$$

In equation (8), k is the Boltzmann constant (in units of eV/K) and E_a is the thermal energy of the trap (in units of eV).

Using the slopes of the linear fits and equation (8), the activation energies (Ea) and frequency factors (s) for the peaks at 90 °C, 140 °C, 210 °C, and 240 °C were calculated and reported in Table 1.

Bacillus pasteurii played an important role in $CaCO_3$ precipitation (Jonkers et al., 2010). It exhibits high urease production. It has been used for microbial calcite cementation in many studies. Calcite crystals are often a major component of limestone, speleothems, corals, etc. During the crystallization of calcite ($CaCO_3$), Pb, Mn, Cu, Mg, and Fe are the main impurities of calcite crystals (Ponnusamy et al., 2004). The structure of calcite is not very complex, but can be difficult to identify. It is described as a NaCl-like arrangement of (Ca) cations and (CO_3) anions (Yildirim et al., 2012). The dose-response experiment was the first part of the study and indicates the relationship between TL intensity and applied dose. For a good dosimeter, a linear relationship is expected in the dose-response relationship. In this study, a linear relationship was observed between 144Gy and 2.3 kGy. Unfortunately, this value is much larger for the personal dosimeter. However, it can be useful as a retrospective dosimeter and can be used in space studies and research laboratories in nuclear reactors. The position of the high TL peaks is not affected by the different values of the applied dose. This result shows that the structure of traps in the high temperature region of the sample is not affected by the variation of the applied dose. High radiation can affect the structure of dosimeters. However, the TL peak of the shallow trap found at ~90 °C disappears at 2.3 kGy, which could be due to the effects of high radiation doses. The TL peak intensity and the normalized area under the TL glow curve decrease with increasing heating rate (Wintle, 1975). explains this situation by the thermal quenching effect. The other reason could be the increased probability of non-radiative transitions at higher temperatures (Topaksu and Yazici, 2007). Reading of irradiated sample at higher heating rate leads to a shift of the TL peak position to higher temperature region. The sample thickness has a great influence on the temperature gradient and temperature lag especially at higher heating rates (Kiyak and Buluş, 2001). Therefore, the measured temperature may differ from the sample temperature which is caused by a small temperature lag due to the thermal contact between the heater and the sample at high heating rates. Therefore, the maximum temperature value read from glow curve becomes lower than that of the heater (Toktamiş and Hama, 2019). The present study shows that the TL peak intensities at 90 °C and 140 °C fade completely after 24 and 336 h storage time, respectively, when the sample is waited in a darkroom. The reduction or loss of TL signal in the sample as a function of time is called fading. Fading is highly dependent on the depth of the traps when the sample read out by a TLD reader. There are many factors that cause the fading process, the main one is temperature and light. In thermal fading, the traps which show lower entrapment energy will decline faster than more energetic ones, because they have higher transition possibility (Toktamiş and Hama, 2019). For a good dosimeter, the same result is required at the end of each repetition of the experiment. Although the standard deviation of the TL peak intensity values is greater than 2% with cycle of measurement, the position of the TL peaks is not affected by the repeat of experiment with small standard deviation (<2%). In addition, the trap depths and frequency factors of each peak (90 °C, 140 °C, 210 °C and 240 °C) were evaluated using the variable heating rate (VHR) method. When a TL glow curve includes small

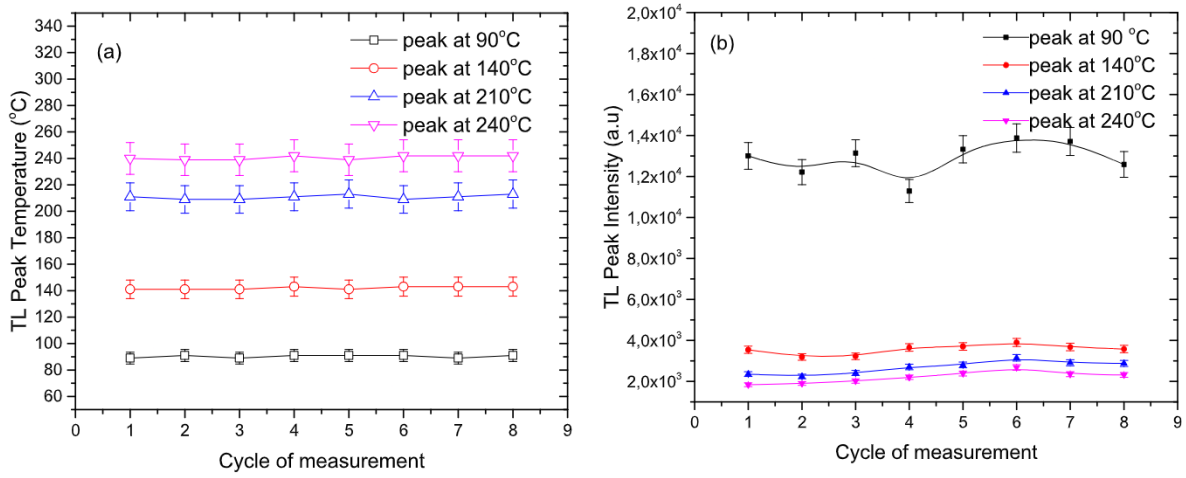

Fig. 10. The variation of (a) TL peak temperatures and (b) TL peak intensities as a function of cycle of measurement.

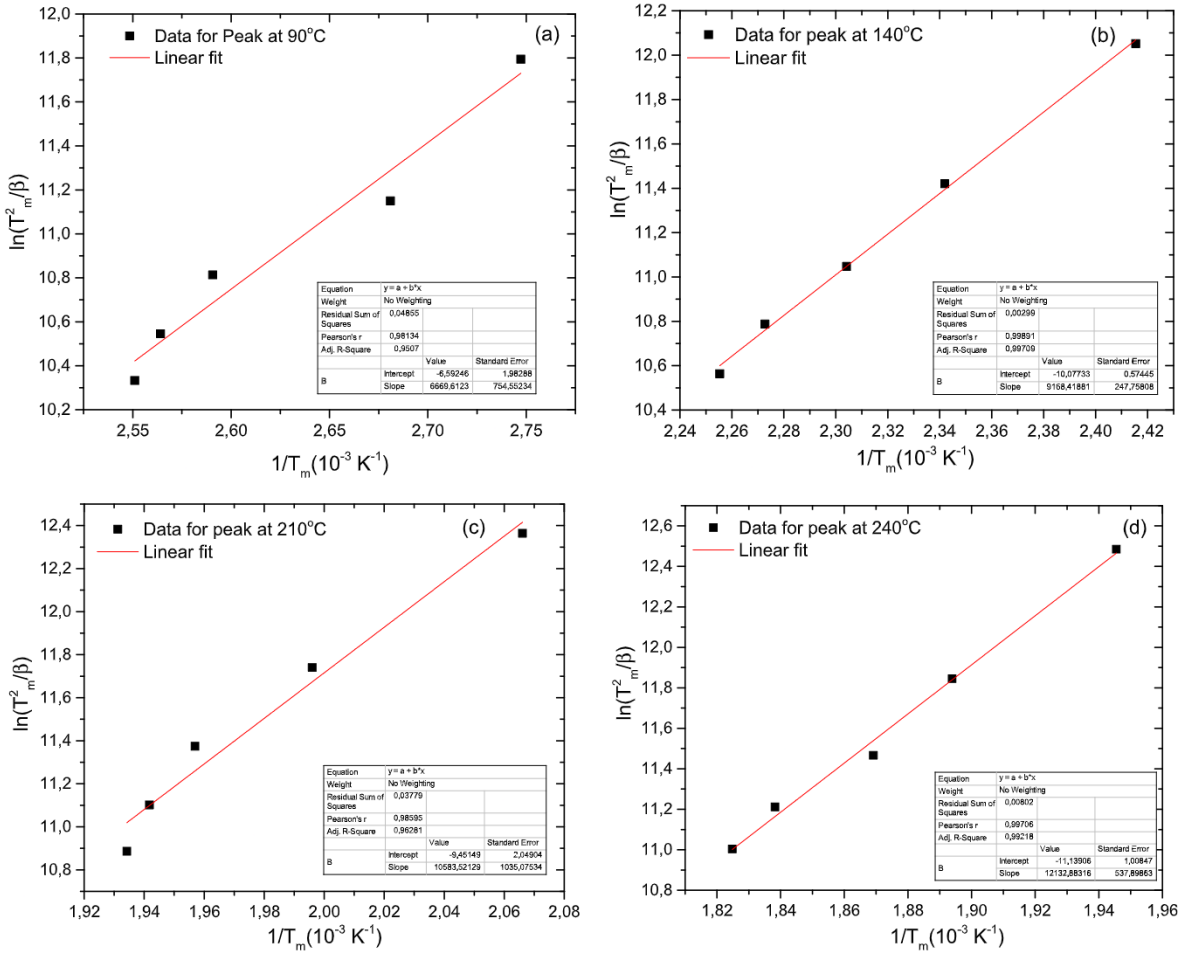

Fig. 11. The graph of ln (T_m^2/β) versus $1/T_m$ of (a) peak at 90 °C, (b) peak at 140 °C, (c) peak at 210 °C and (d) peak at 240 °C.

Table 1
Calculated activation energies (E_a) and frequency factors (s) for peaks at 90 °C, 140 °C, 210 °C and 240 °C via variable heating rate (VHR).

	Peak at 90 °C	Peak at 140 °C	Peak at 210 °C	Peak at 240 °C
E_a (eV)	0.574	0.79	0.911	1.045
s (s^{-1})	4.86×10^9	2.16×10^{11}	1.41×10^{11}	8.27×10^{11}

satellite peaks surrounding the main peak, the VHR method becomes very useful for calculating the kinetic parameters because it has little effect on the accuracy of the kinetic parameters. Temperature lag (TLA) is one of the reasons for poor estimation of kinetic parameters (Yazici and Topaksu, 2003). This is the temperature difference between the heating element and the sample during TL readout.

5. Conclusion

In this study, the thermoluminescence properties of calcite conducted by bacterial calcium carbonate ($CaCO_3$) precipitation (BCCP) in organic soil were investigated. The calcite sample conducted by bacterial calcium carbonate ($CaCO_3$) precipitation (BCCP) in organic soil shows good TL properties in terms of wide linear dose-response range, good reproducibility and high stability of dosimetric peaks with low fading. It has a clear TL glow curve with four distinct peaks located at 90 °C, 140 °C, 210 °C and 240 °C. It is known that 90 °C peak is not used in the dosimetric studies because the ambient temperature and light highly affect charge carriers trapped at shallow traps. A desirable property of TL dosimetry is the wide linear relationship between TL intensity and absorbed dose (McKeever, 1985). In the dose range of 140Gy and 2.3 kGy, a linear dose-response was observed. This linear dose response is seen at higher dose region and may be used as a high dose dosimetry such as in space studies and in nuclear reactors. The sample has a good reusability due to the stabilities of TL peak intensities (140, 210, and 240 °C) after eight cycle of measurements. For a good dosimeter, low fading characteristic of the TL dosimeter is desired. The area under the TL peaks between 30 °C –150 °C decreases suddenly up to 100 min of storage time and finally faded completely. This is an expected result because of shallow traps but the area between 150 and 400 °C seems almost constant. The activation energies (E_a) and frequency factors (s) for peaks at 90 °C, 140 °C, 210 °C and 240 °C were evaluated via variable heating rate (VHR). The activation energies (E_a) and frequency factor (s) of the peaks in the TL glow curve are lying between 0.57eV and 1.04 eV; 4.86×10^9 and 8.27×10^{11}, respectively.

CRediT authorship contribution statement

Hüseyin Toktamış: Investigation. **Muhammed Hatib:** Investigation. **H. İbrahim Kılıç:** Investigation. **Hanifi Çanakçı:** Investigation.

Declaration of competing interest

The authors declare that they have no known competing financial interests or personal relationships that could have appeared to influence the work reported in this paper.

Data availability

Data will be made available on request.

References

Anbu, P., Kang, C.H., Shin, Y.J., So, J.S., 2016. Formations of calcium carbonate minerals by bacteria and its multiple applications. Springer plus 5 (1), 1–26. https://doi.org/10.1186/s40064-016-1869-2.

Barkay, T., Schaefer, J., 2001. Metal and radionuclide bioremediation: issues, considerations and potentials. Curr. Opin. Microbiol. 4 (3), 318–323. https://doi.org/10.1016/s1369-5274(00)00210-1.

Benzerara, K., Miot, J., Morin, G., Ona-Nguema, G., Skouri-Panet, F., Ferard, C., 2011. Significance, mechanisms and environmental implications of microbial biomineralization. Compt. Rendus Geosci. 343 (2–3), 160–167. https://doi.org/10.1016/j.crte.2010.09.002.

Bos, A.J.J., 2007. Theory of thermoluminescence. Radiat. Meas. 41, 45–56. https://doi.org/10.1016/j.radmeas.2007.01.003.

Bosak, T., 2011. Calcite precipitation, microbially induced. In: Reitner, J., Thiel, V. (Eds.), Encyclopedia of Earth Sciences Series. Springer, Netherlands, pp. 223–227.

Calderon, T., Townsend, P.D., Beneitez, P., Garcia-Guinea, J., Millan, A., Rendell, H.M., Tookey, A., Urbina, M., Wood, R.A., 1996. Crystal field effects on the thermoluminescence of manganese in carbonate lattices. Radiat. Meas. 26 (5), 719–731. https://doi.org/10.1016/S1350-4487(97)82886-7.

Chen, R., McKeever, S.W., 1997. Theory of Thermoluminescence and Related Phenomena. World Scientific. https://doi.org/10.1142/2781.

Claudio, F., 2003. Handbook of Thermoluminescence. https://doi.org/10.1142/5167.

De Muynck, W., De Belie, N., Verstraete, W., 2010. Microbial carbonate precipitation in construction materials: a review. Ecol. Eng. 36 (2), 118–136. https://doi.org/10.1016/j.ecoleng.2009.02.006.

DeJong, J.T., Mortensen, B.M., Martinez, B.C., Nelson, D.C., 2010. Bio-mediated soil improvement. Ecol. Eng. 36 (2), 197–210. https://doi.org/10.1016/j.ecoleng.2008.12.029.

Dhami, N.K., Reddy, M.S., Mukherjee, A., 2013. Biomineralization of calcium carbonate polymorphs by the bacterial strains isolated from calcareous sites. J. Microbiol. Biotechnol. 23 (5), 707–714. https://doi.org/10.4014/jmb.1212.11087.

Douglas, S., Beveridge, T.J., 1998. Mineral formation by bacteria in natural microbial communities. FEMS Microbiol. Ecol. 26 (2), 79–88. https://doi.org/10.1111/j.1574-6941.1998.tb00494.x.

Duller, G.A.T., Penkman, K.E.H., Wintle, A.G., 2009. Assessing the potential for using biogenic calcites as dosemeters for luminescence dating. Radiat. Meas. 44 (5–6), 429–433. https://doi.org/10.1016/j.radmeas.2009.02.008.

Garcia-Guinea, J., Crespo-Feo, E., Correcher, V., Cremades, A., Rubio, J., Tormo, L., Townsend, P.D., 2009a. Luminescence of strontianite (SrCO3) from strontian (Scotland, UK). Radiat. Meas. 44 (4), 338–343. https://doi.org/10.1016/j.radmeas.2009.03.018.

Garcia-Guinea, J., Crespo-Feo, E., Correcher, V., Rubio, J., Roux, M.V., Townsend, P.D., 2009b. Thermo-optical detection of defects and decarbonation in natural smithsonite. Phys. Chem. Miner. 36, 431–438. https://doi.org/10.1007/s00269-009-0289-z.

García-Guinea, J., Correcher, V., Benavente, D., Sanchez-Moral, S., 2015. Composition, luminescence, and color of a natural blue calcium carbonate from Madagascar. Spectrosc. Lett. 48 (2), 107–111. https://doi.org/10.1080/00387010.2013.857692.

Gómez-Ros, J.M., Kitis, G., 2002. Computerised glow curve deconvolution using general and mixed order kinetics. Radiat. Protect. Dosim. 101, 47–52. https://doi.org/10.1093/oxfordjournals.rpd.a006029.

Gómez-Ros, J.M., Furetta, C., Correcher, V., 2006. Simple methods to analyse thermoluminescence glow curves assuming arbitrary recombination–retrapping rates. Radiat. Protect. Dosim. 119 (1–4), 339–343. https://doi.org/10.1093/rpd/nci523.

Horowitz, Y.S., Yossian, D., 1995. Computerised glow curve deconvolution: application to thermoluminescence dosimetry. Radiat. Protect. Dosim. 60, 5–12. https://doi.org/10.1093/oxfordjournals.rpd.a082702.

Isik, E., Toktamis, D., Er, M.B., Hatib, M., 2021. Classification of thermoluminescence features of CaCO3 with long short-term memory model. Luminescence 36 (7), 1684–1689. https://doi.org/10.1002/bio.4109.

Jonkers, H.M., Thijssen, A., Muyzer, G., Copuroglu, O., Schlangen, E., 2010. Application of bacteria as self-healing agent for the development of sustainable concrete. Ecol. Eng. 36 (2), 230–235. https://doi.org/10.1016/j.ecoleng.2008.12.036.

Kiyak, N.G., Buluş, E., 2001. Effect of annealing temperature on determining trap depths of quartz by various heating rates method. Radiat. Meas. 33 (6), 879–882. https://doi.org/10.1016/S1350-4487(01)00248-7.

Konishi, Y., Tsukiyama, T., Ohno, K., Saitoh, N., Nomura, T., Nagamine, S., 2006. Intracellular recovery of gold by microbial reduction of AuCl4− ions using the anaerobic bacterium Shewanella algae. Hydrometallurgy 81 (1), 24–29. https://doi.org/10.1016/j.hydromet.2005.09.006.

Krbetschek, M.R., Gotze, J., Dietrich, A., Trautmann, T., 1997. Spectral information from minerals relevant for luminescence dating. Radiat. Meas. 27, 695–748. https://doi.org/10.1016/S1350-4487(97)00223-0.

Lowenstam, H.A., 1981. Minerals formed by organisms. Science 211 (4487), 1126–1131. https://doi.org/10.1126/science.7008198.

Lowenstam, H.A., Weiner, S., 1989. On Biomineralization. Oxford University Press. https://doi.org/10.1093/oso/9780195049770.001.0001.

McKeever, S.W.S., 1985. Thermoluminescence of Solids. Cambridge University Press, Cambridge. https://doi.org/10.1017/CBO9780511564994.

Pagonis, V., Kitis, G., Furetta, C., 2006. Numerical and Practical Exercises in Thermoluminescence. Springer Science & Business Media. https://doi.org/10.1007/0-387-30090-2.

Phillips, A.J., Gerlach, R., Lauchnor, E., Mitchell, A.C., Cunningham, A.B., Spangler, L., 2013. Engineered applications of ureolytic biomineralization: a review. Biofouling 29 (6), 715–733. https://doi.org/10.1080/08927014.2013.796550.

Polikreti, K., Michael, C.T., Maniatis, Y., 2003. Thermoluminescence characteristics of marble and dating of freshly excavated marble objects. Radiat. Meas. 37 (1), 87–94. https://doi.org/10.1016/S1350-4487(02)00088-4.

Ponnusamy, V., Ramasamy, V., Dheenathayalu, M., Hemalatha, J., 2004. Effect of annealing in thermostimulated luminescence (TSL) on natural blue colour calcite crystals. Nucl. Instrum. Methods Phys. Res. Sect. B Beam Interact. Mater. Atoms 217 (4), 611–620. https://doi.org/10.1016/j.nimb.2003.12.037.

Rodriguez-Navarro, C., Jroundi, F., Schiro, M., Ruiz-Agudo, E., González-Muñoz, M.T., 2012. Influence of substrate mineralogy on bacterial mineralization of calcium carbonate: implications for stone conservation. Appl. Environ. Microbiol. 78 (11), 4017–4029. https://doi.org/10.1128/AEM.07044-11.

Schaetzl, R.J., Anderson, S., 2005. Soils: Genesis and Geomorphology. Cambridge Univ Pr.

Sıdık, W., Canakcı, H., Kılıc, I.H., 2015. An investigation of bacterial calcium carbonate precipitation in organic soil for geotechnical applications. Iranian J. Sci. Technol. Transact. Civil Eng. 39 (C1), 201–205.

Stocks-Fischer, S., Galinat, J.K., Bang, S.S., 1999. Microbiological precipitation of CaCO3. Soil Biol. Biochem. 31 (11), 1563–1571. https://doi.org/10.1016/S0038-0717(99)00082-6.

Tatumi, S.H., Nagatomo, T., Matsuoka, M., Watanabe, S., 1993. Thermoluminescence and ESR in an aragonite speleothem. J. Phys. Appl. Phys. 26 (9), 1482–1486. https://doi.org/10.1088/0022-3727/26/9/022.

Toktamış, D., Toktamış, H., Yazıcı, A.N., 2016. The effects of thermal treatments on the thermoluminescence properties of biogenic minerals present in the seashells. Radiat. Eff. Defect Solid 171 (11–12), 951–964. https://doi.org/10.1080/10420150.2016.1259623.

Toktamiş, H., Hama, P.O., 2019. Thermoluminescence dosimetric properties of silicon carbide (SiC) used in industrial applications. Appl. Radiat. Isot. 148, 138–146. https://doi.org/10.1016/j.apradiso.2019.03.036.

Toktamiş, H., Toktamiş, D., Yazici, A.N., 2014. Thermoluminescence studies of calcite extracted from natural sand used in making roasted chickpea. J. Lumin. 153, 375–381. https://doi.org/10.1016/j.jlumin.2014.03.061.

Topaksu, M., Yazici, A.N., 2007. The thermoluminescence properties of natural CaF2 after β-irradiation. Nucl. Instrum. Methods Phys. Res. Sect. B Beam Interact. Mater. Atoms 264 (2), 293–301. https://doi.org/10.1016/j.nimb.2007.09.018.

Topaksu, M., Correcher, V., Garcia-Guinea, J., Yüksel, M., 2015. Effect of heating rate on the thermoluminescence and thermal properties of natural ulexite. Appl. Radiat. Isot. 95, 222–225. https://doi.org/10.1016/j.apradiso.2014.10.020.

Valle-Fuentes, F.J., Garcia-Guinea, J., Cremades, A., Correcher, V., Sanchez-Moral, S., Gonzalez-Martin, R., et al., 2007. Low-magnesium uranium–calcite with high degree of crystallinity and gigantic luminescence emission. Appl. Radiat. Isot. 65 (1), 147–154. https://doi.org/10.1016/j.apradiso.2006.07.010.

Wintle, A.G., 1975. Thermal quenching of thermoluminescence in quartz. Geophys. J. Int. 41 (1), 107–113. https://doi.org/10.1111/j.1365-246X.1975.tb05487.x.

Yazici, A.N., Topaksu, M., 2003. The analysis of thermoluminescence glow peak of unannealed synthetic quartz. J. Phys. D Appl. Phys. 36, 620–627. https://doi.org/10.1088/0022-3727/36/6/303.

Yildirim, R.G., Kafadar, V.E., Yazici, A.N., Gün, E., 2012. The analysis of thermoluminescent glow peaks of natural calcite after beta irradiation. Radiat. Protect. Dosim. 151 (3), 397–402. https://doi.org/10.1093/rpd/ncs020.

Yoshida, N., Higashimura, E., Saeki, Y., 2010. Catalytic biomineralization of fluorescent calcite by the thermophilic bacterium Geobacillus thermoglucosidasius. Appl. Environ. Microbiol. 76 (21), 7322–7327. https://doi.org/10.1128/AEM.01767-10.